9

Superhydrophobic Superoleophobic Woven Fabrics

Hoonjoo Lee[1] and Jeffery Owens[2]
[1]*North Carolina State University*
[2]*Air Force Research Laboratory*
U.S.A.

1. Introduction

Technologies related to superhydrophobic and superoleophobic treatments have recently attracted considerable attention in the textile industry due to their potential applications in medical devices as well as industrial materials. A surface whose water contact angle exceds150° is called a superhydrophobic surface, and we define a surface with an oil contact angle of over 150° as a superoleophobic surface. Since the wettability of a solid surface is determined by two parameters, the chemical composition and the geometrical structure of a rough surface, the combination of these two factors are often used to design superhydrophobic and superoleophobic textiles. More specifically researchers employ two predominant rough surface wetting models, the Wenzel model and the Cassie–Baxter model compared to the wetting behaviour of a smooth surface to predict the requirements for imparting a fabric with superhydrophobic and superoleophobic character. However, not all surfaces having high contact angles to liquids possess low roll-off angles. Rather, roll-off angles are highly dependent on the mass and density of the droplet, the surface tensions of both the liquid and the surface the droplet is sitting atop of, and the geometrical morphology and degree of roughness of that surface. Typically, unless a surface possesses a very low surface tension that is approximately one forth the surface tension of the liquid, droplets of less than 50 μL are not mobile when the surface is tilted.

In this chapter, the relationships amongst contact angles, surface tension, and surface roughness are reviewed; the wetting behaviour of a rough surface is compared with that of a smooth surface; the relationships between contact angle hysteresis and roll-off angles are analysed, and finally superhydrophobic, superoleophobic woven fabric is designed and developed using chemical and geometrical surface modifications.

2. Design and preparation of superhydrophobic superoleophobic woven fabric

Although it is hard to measure the surface tension of a solid directly, it is easy to measure the contact angles of liquid droplets sitting atop its surface (Fig. 1). By obtaining the contact angle data for liquids with varying surface tensions and inserting the data into select equations predictions of a surface's wetting characteristics to other liquids can be obtained.

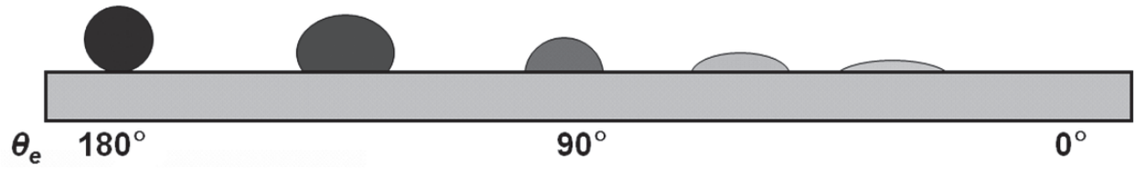

Fig. 1. Contact angle and wettability

2.1 Wetting behavior of smooth and rough surfaces

The relationship between surface tension and contact angle is obtained by the Young equation:

$$\frac{\gamma_{SV} - \gamma_{SL}}{\gamma_{LV}} = \cos\theta_e \tag{1}$$

where γ is the surface tension; and SV, SL, and LV are the solid-vapour, the solid-liquid, and the liquid-vapour interfaces, respectively (Fig. 2). According to Young's equation, the contact angle is a well-defined property that depends on the surface tension coefficients that exist between the solid−liquid and the liquid−gas interface.

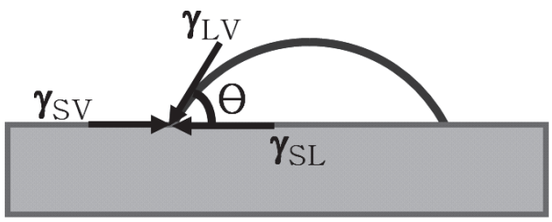

Fig. 2. A drop on a flat surface

The right hand side of equation (1) and γ_{LV} can be obtained from experimental measurements, leaving two unknowns, γ_{SV} and γ_{SL}. When θ_e for a test liquid is> 20°, it is assumed that $\gamma_{SV} \approx \gamma_S$ and $\gamma_{LV} \approx \gamma_L$. On the other hand, the thermodynamic work of adhesion, $W_{SL}{}^a$ can be explained by the Dupre equation as:

$$W_{SL}^a = \gamma_{SV}^a + \gamma_{LV}^a - \gamma_{SL}^a \tag{2}$$

Combining equation (1) and (2) results in the Dupre-Young equation:

$$W_{SL}^a = \gamma_{SV}^a + \gamma_{LV}^a - \gamma_{SL}^a = \gamma_{LV}^a(1 + \cos\theta_e) \tag{3}$$

According to Fowkes, when only dispersion interactions are present, the interfacial tension between the solid and liquid is $\gamma_{SL}^{LW} = (\sqrt{\gamma_{SV}^{LW}} - \sqrt{\gamma_{LV}^{LW}})^2$ and the geometric mean of the liquid and solid surface tension is:

$$W_{SL}^{LW} = 2\sqrt{\gamma_{SV}{}^{LW}\gamma_{LV}{}^{LW}} \tag{4}$$

where $W_{SL}{}^{LW}$ is the thermodynamic work of Lifshitz–van der Waals (LW) components.
Meanwhile, the addition of intermolecular forces at the interface is equal to the surface tension of the material, as shown in equation (5).

$$\gamma = \gamma^{d} + \gamma^{p} + \gamma^{H} + \gamma^{ind} + \gamma^{m} + \ldots \quad (5)$$

where d, p, H, ind, and m mean London dispersion forces, permanent dipoles, hydrogen bonds, induced dipoles and metallic interaction, respectively. Therefore, we can determine γ_{SV} and γ_{LV} as:

$$\gamma_{SV} = \gamma_{SV}^{d} + \gamma_{SV}^{p} + \gamma_{SV}^{H} + \gamma_{SV}^{ind} + \gamma_{SV}^{m} + \ldots \quad (6)$$

$$\gamma_{LV} = \gamma_{LV}^{d} + \gamma_{LV}^{p} + \gamma_{LV}^{H} + \gamma_{LV}^{ind} + \gamma_{LV}^{m} + \ldots \quad (7)$$

Combining equation (3), (4), (6) and (7) gives:

$$\begin{aligned} &\gamma_{LV}(1+\cos\theta_e) \\ &= \gamma_{LV}^{d}(1+\cos\theta_e) + \gamma_{LV}^{p}(1+\cos\theta_e) + \gamma_{LV}^{H}(1+\cos\theta_e) + \gamma_{LV}^{ind}(1+\cos\theta_e) + \gamma_{LV}^{m}(1+\cos\theta_e) + \ldots \\ &= 2(\sqrt{\gamma_{SV}^{d}\cdot\gamma_{LV}^{d}} + \sqrt{\gamma_{SV}^{p}\cdot\gamma_{LV}^{p}} + \sqrt{\gamma_{SV}^{H}\cdot\gamma_{LV}^{H}} + \sqrt{\gamma_{SV}^{ind}\cdot\gamma_{LV}^{ind}} + \sqrt{\gamma_{SV}^{m}\cdot\gamma_{LV}^{m}} + \ldots) \end{aligned} \quad (8)$$

Since the surface tensions of dodecane and most polymeric surfaces are determined by London dispersion forces, this equation can be simplified to:

$$\gamma_{LV}(1+\cos\theta_e) = 2(\sqrt{\gamma_{SV}^{d}\cdot\gamma_{LV}^{d}}) \quad (9)$$

An oil, such as dodecane has a very low surface tension, ~24.5 dyne/cm. Substituting γ_L = 24.5 dyne/cm for dodecane into Eq. 9 suggests γ_S must be smaller than 6.3 dyne/cm, and a smooth surface having $\gamma_{SV} \leq 6.3$ dyne/cm is oleophobic ($\theta_e > 90^o$) under these conditions. The Young equation and Dupre-Young equation are valid only for the wetting of smooth surfaces, but real solids are not perfectly flat and surface structure greatly effects wettability, e.g. when a rough surface of a solid is very hydrophobic, liquid droplets are in contact with the upper part of a rough surface and the lower part is filled with air.

In order to design a superhydrophobic superoleophobic surface, two predominant rough wetting models are used: the Wenzel model and the Cassie–Baxter model. In the Wenzel model a liquid fills the grooves of a rough surface and completely wets the surface, whilst in the Cassie–Baxter model, a liquid sits on top of the surface and repels the liquid. To create a Cassie–Baxter surface, the Young contact angle of a liquid, θ_e, must be greater than 90^o as shown in Fig. 3.

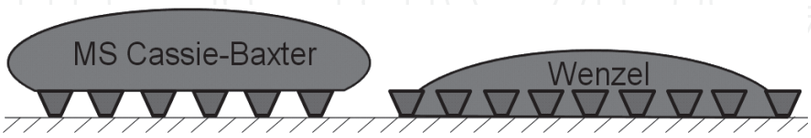

Fig. 3. A drop on a rough surface

In Wenzel's approach the liquid fills the grooves on the rough surface, and the liquid contact angle on a rough surface, θ_r^W, can be described as:

$$\cos\theta_r^{W} = r\cos\theta_e \quad (10)$$

where r is roughness — the ratio of the total wet area of a rough surface to the apparent surface area in contact with the water droplet (r > 1). According to equation (10), for a rough

surface (r > 1) a hydrophilic surface becomes more hydrophilic while a hydrophobic surface does more hydrophobic, e.g. for a material with $\theta_e \approx 120^o$, r must be greater than 1.79 to make the surface superhydrophobic. Since most solid surfaces typically possess $\gamma_{SV} > 6.3$ dyne/cm, the Cassie–Baxter model does not allow for stable superoleophobicity under normal circumstances. On a metastable Cassie–Baxter surface, a liquid initially sits atop of the surface since air pockets inside the grooves of the rough surface provides lower Gibbs free energy than that when the liquid penetrates the rough surface. However, the liquid can be potentially drawn into contact with the rough surface over time, with the time to absorption dependent on the surface tension, volume, and density of the liquid, and the surface tension and morphology of the surface. Hence, a superoleophobic surface can be produced by designing a metastable Cassie–Baxter surface.

The Cassie and Baxter model is an extended form of the Wenzel model to include porous surfaces. In this model a liquid sits on a composite surface made of a solid and air. Therefore, the liquid does not fill the grooves of a rough solid. In their paper published in 1944, Cassie and Baxter suggested that the liquid contact angle at on such a rough surface, θ_r^{CB}, is:

$$\cos\theta_r^{CB} = f_1\cos\theta_e - f_2 \tag{11}$$

where f_1 is the surface area of the liquid in contact with the solid divided by the projected area, and f_2 is the surface area of the liquid in contact with air trapped in the pores of the rough surface divided by the projected area. When there is no trapped air, f_1 is the same with r in the Wenzel model. In the Cassie-Baxter model, the smooth surface can become more hydrophobic or oleophobic by surface roughening, regardless of θ_e. However, in the Wenzel model, θ_e has to be greater than 90^o in order for a smooth surface to be more hydrophobic or oleophobic after roughening. This statement reinforces the concept of the metastable Cassie–Baxter model, i.e. a surface having $\theta_e < 90^o$ with a liquid, when roughened, will immediately wet (Wenzel behaviour) or the liquid will sit on top of the surface due to air pockets inside the grooves which result in a local minimum in the surface energy (meta-stable Cassie-Baxter behaviour). In addition, since the surface tension of an oil such as dodecane is lower than that of water (γ = 72.8 dyne/cm), the θ_r^{CB} of water is higher than θ_r^{CB} of oil. Hence, according to equations (10) and (11), all superoleophobic surfaces should be superhydrophobic, but not all superhydrophobic surfaces exhibit superoleophobicity.

2.2 Preparation of superhydrophobic and superoleophobic woven fabric

Superhydrophobicity has gained a great deal of interest and has been studied extensively since one of the most-prized features of superhydrophobic surfaces is their ability to self-clean — that is the ability of water to collect and remove dirt and debris as the water droplet rolls off of the surface. The roll-off angle of a droplet, α, on a smooth surface can be described as:

$$mg\sin\alpha \approx -2R_w\gamma_{LV}(\cos\theta_A - \cos\theta_R) \tag{12}$$

where m is the mass of the droplet, g is the gravitational acceleration, R_w is the radius of the wetting area, θ_A is the advancing contact angle, and θ_R is the receding contact angle. Meanwhile, contact angle hysteresis, $\Delta\theta_H$, is defined as the difference between advancing and receding contact angles, i.e. $\Delta\theta_H = \theta_A - \theta_R$. The gain factor, which is often used to

understand the relationship between contact angle hystereses and roll-off angle, is considered as the rate of variation of the contact angle hysteresis at any operating point. The radius of the wetting area, R_w, on a surface is:

$$R_w = \sqrt[3]{\frac{3V}{\pi(2-3\cos\theta+\cos^3\theta)}}x\sin\theta \tag{13}$$

Based on equation (13), the radius of the wetting area can be predicted as shown in Table 1.

θ (°)	R_c (mm)			
	5μL	10 μL	20 μL	50 μL
10	3.31	4.17	5.26	7.14
20	2.62	3.30	4.15	5.63
30	2.27	2.85	3.60	4.88
40	2.03	2.56	3.23	4.38
50	1.86	2.34	2.94	4.00
60	1.71	2.15	2.71	3.68
70	1.58	1.99	2.50	3.40
80	1.46	1.83	2.31	3.13
90	1.34	1.69	2.12	2.88
100	1.22	1.54	1.94	2.63
110	1.10	1.39	1.75	2.37
120	0.97	1.23	1.55	2.10
130	0.84	1.06	1.33	1.81
140	0.69	0.87	1.10	1.49
150	0.54	0.67	0.85	1.15
160	0.37	0.46	0.58	0.78
170	0.19	0.23	0.29	0.40

Table 1. Radius of wetting area of liquid droplets

The Wenzel equation gives a change in the Wenzel contact angle, $\Delta\theta_H^W$, caused by a change in the contact angle on the smooth surface, $\Delta\theta_H$, as:

$$\Delta\theta_H^W = r\left(\frac{\sin\theta_e}{\sin\theta_r^W}\right)\Delta\theta_H \tag{14}$$

The gain factor, which is the change in $\cos\theta_r^W$ relative in $\cos\theta_e$ (i.e. the derivative of $\cos\theta_r^W$ with respect to $\cos\theta_e$) is very useful since it separates the idea of the equilibrium contact angle increase occurring by surface topography from the observed contact angle. Using the Wenzel equation we can obtain the Wenzel gain factor as follows:

$$G_e^W = \frac{r\sin\theta_e}{\sin\theta_r^W} \tag{15}$$

Since the effect of roughness is proportional to the radian contact angle changes, the Wenzel gain factor is approximately unity when a contact angle θ_e is close to 90°, but the Wenzel

gain factor rapidly increases as the roughness factor increases. Likewise, Cassie-Baxter equation gives a change in the Cassie-Baxter contact angle, $\Delta\theta_H^{CB}$, caused by a change in the contact angle on the smooth surface, $\Delta\theta_H$, as:

$$\Delta\theta_H^{CB} = (1 - f_2)\left(\frac{\sin\theta_e}{\sin\theta_r^{CB}}\right)\Delta\theta_H \tag{16}$$

Similarly, a Cassie-Baxter gain factor, G_e^{CB}, can be obtained by the Cassie-Baxter equation as:

$$G_e^{CB} = (1 - f_2)\left(\frac{\sin\theta_e}{\sin\theta_r^{CB}}\right) \tag{17}$$

Since $1 - f_2 \leq 1$, $G_e^{CB} \leq 1$. According to McHale, the Cassie-Baxter gain factor, G_e^{CB}, is an attenuation of any contact angle hysteresis, whilst hysteresis increases on a Wenzel-type surface. As a numerical example, if a water droplet is deposited on a rough nylon surface having $\theta_e = 68°$, $\Delta\theta_H = 150°$ and r = 3, the apparent contact angle, θr^W, will be ~ 0° and thus the contact angle hysteresis on this Wenzel surface, $\Delta\theta_H^W$, will be greater than 150°, i.e., the droplet will be adsorbed onto the rough structure and will not be able to roll off such a hydrophilic rough surface. However, if a water droplet is deposited on a poly(tetrafluoroethylene) (PTFE) having θe = 120°, $\Delta\theta_H = 80°$ and $f_2 = 0.74$, the apparent contact angle, θ_r^{CB}, will be 150° and the contact angle hysteresis, $\Delta\theta_H^{CB}$, on this C−B surface will be less than 80°, i.e. the surface will become superhydrophobic and liquid droplets will readily roll off at a certain roll-off angle. In the case of dodecane, whose $\theta_e < 90°$ and $\theta_r^{CB} > 90°$, the situation is less favorable, and equations (16) and (17) cannot be used to predict α of dodecane since the sine curve has a bilateral symmetry with respect to 90°. Hence, equations (16) and (17) have to be modified for a metastable CB surface as:

$$\Delta\theta_H^{\text{metastable-CB}} = (1 - f_2)\left(\frac{1 + \cos\theta_e}{1 + \cos\theta_r^{CB}}\right)\Delta\theta_H \tag{18}$$

$$G_e^{\text{metastable-CB}} = (1 - f_2)\left(\frac{1 + \cos\theta_e}{1 + \cos\theta_r^{CB}}\right) \tag{19}$$

Hence, if there is a surface having surface properties as shown in Table 2, α can be predicted by equations (12), (16), and (18).

The predicted values of α are 15° and 10° for 50 μL and 100 μL water droplets, and 45° and 26° for 50 μL and 100 μL dodecane droplets, respectively. If liquids having different γ_{LV} are deposited on a solid surface, the roll-off angles of the liquids are strongly influenced by the mass and the surface energy of each liquid.

2.3 Preparation of superhydrophobic and superoleophobic woven fabric

Again, the wettability of a solid surface is determined by two parameters: the chemical composition and the geometrical structure of a rough surface. Therefore, in this chapter, we design a metastable superoleophobic surface via chemical and geometrical modifications. The surface energy of the fibres are reduced by grafting 1,1,2,2,-tetrahydrodecyltrimethoxysilane (FS) onto nylon and cotton fibres composing nylon cotton

Parameters	Water on PTFE (CB)		Dodecane on PTFE (metastable CB)	
	50 μL	100 μL	50 μL	100 μL
θ_e (°)	120	120	50	50
$\Delta\theta_H$ (°)	110	110	168	168
f_2	0.74	0.74	0.74	0.74
θ_r^{CB} (°)*	150	150	124	124
$\Delta\theta_H^{CB}$ (°)	50	50	163	163
θ_A^{CB} (°)	180	180	180	180
θ_R^{CB} (°)	30	30	17	17
R_w (mm)	2.5	3.3	3.7	4.5
α (°)	**15**	**10**	**45**	**26**

* Approximate values if $f_1 + f_2 \sim 1$.

Table 2. Predicted roll-off angles of water and dodecane on a very hydrophobic and oleophobic rough surface. Here, since the droplet shape begins to deform when m > 10 μL caused by gravity, we use real R_w that is not a predicted value based on equation (13) but a real R_c which has been measured on the surface.

blended woven fabric (NyCo). Macro scale roughness of the NyCo can be controlled via choice of fabric construction, yarn type (mono or multi-filament), and fibre diameter. Additionally, micro and nano scale roughness on the fibres can be achieved by allowing partial condensation of the FS prior to treating the NyCo, thus resulting in deposition of FS particulate condensates over the fibre surface. First, we review how to lower the surface tension of fibres chemically.

2.3.1 Chemical modification

Lowering surface tension of NyCo begins by grafting low-surface-tension material on the surface of NyCo such as replicating the FS grafting process developed by Hoefnagels et al., and Stoeber et al. except that the technique was modified to use microwave radiation in this research. A swatch of NyCo fabric is saturated in a solution containing FS, squeezed at 100 % wet pick-up to remove excess liquid, and cured in a conventional microwave oven at 1250 W, with irradiation times varying time from 0 to 60 sec. Whilst the surface energy of NyCo decreases by FS grafting, silane can form micro- and nano-scale roughness on NyCo and create a high surface area if the FS imparts particulate condensation to the NyCo — the self-condensation of FS will be discussed later in this chapter. Such treatment methods correlate easily to a wide variety of textiles that have –OH and –NH groups such as cotton, polyamides, polyaramids, etc. Fluoroalkyl chains can be attached to the –OH or –NH site via a siloxane or silazane linkage as shown in Fig. 4.

where XH is —OH, —SH, —NH—, and —NH_2, etc. Use of microwave radiation in this process greatly enhances the reaction rate of the covalent attachment of silanes to the reactive substrates, as does the presence of acid or base. Since treatment at low pH is avoided for the treatment of cotton and other cellulose derivatives due to the instability of the β-acetal bonds in acidic solutions, this reaction was processed using neutral and basic solutions.

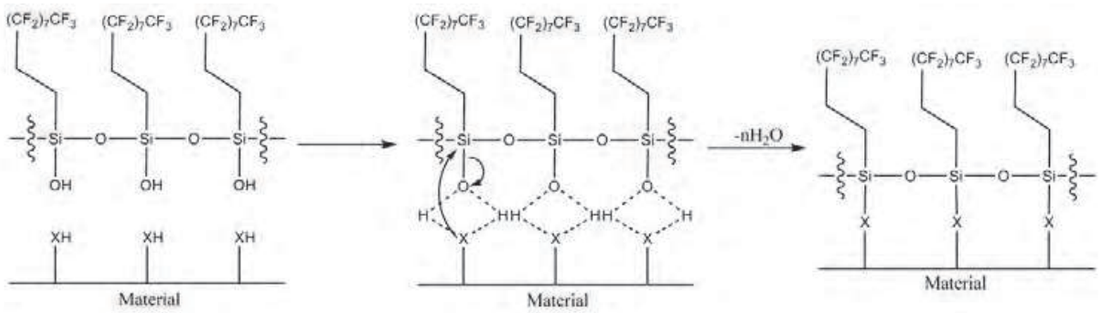

Fig. 4. Reaction mechanism of FS condensation onto a surface

Again, we chemically grafted FS onto a NyCo surface to reduce the surface tension of NyCo and to make the surface less oleophilic. In order to obtain the Young contact angles for water and dodecane, nylon 6,6 film was treated with FS. The Young contact angles of water on a FS-grafted nylon film were 109° – 112°, whilst the Young contact angles for water on an unmodified nylon surface were 70° – 73°. Grafting FS to a nylon film also increased dodecane contact angles. The Young contact angles for dodecane on a FS-grafted nylon film were 73° – 75°, whilst the Young contact angle for dodecane on an unmodified nylon surface was < 5°. The measured values of $\theta_{e\text{-}water}$ and $\theta_{e\text{-}dodecane}$ on FS-treated nylon are critical parameters to consider when designing superoleophobic surfaces using the Wenzel and Cassie–Baxter models. FS-grafting onto a nylon film successfully generated a surface having a low surface energy, as shown in Fig. 5.

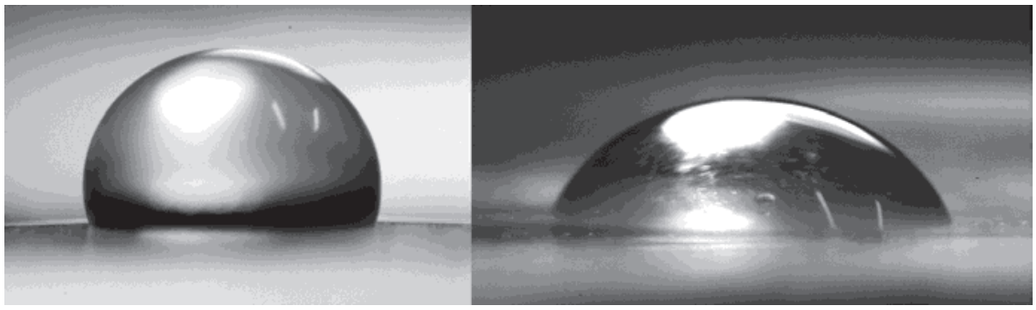

Fig. 5. 10 μL water and dodecane droplets on a FS-grafted nylon film

2.3.2 Geometrical modifications

The wetting behavior of a solid surface is also controlled by the geometrical structure of a surface as mentioned in the beginning of this chapter. In this section, we study how to model and modify a rough surface to make the surface highly hydrophobic and oleophobic using plain woven, woven twill, and 3/1 satin woven constructions.

2.3.2.1 Superhydrophobic oleophobic plain woven structure

To obtain the true surface area we use a flux integral. Fig. 6 shows a cross-sectional view of a model of a NyCo plain woven fabric made of monofilament fibres. The distance from the centre of a weft (or warp) yarn to the centre of an adjacent weft (or warp) yarn is 4R; and the distance from the centre of a weft (or warp) yarn to the centre of an adjacent warp (or weft) yarn is 2R. Hence, according to the Pythagorean Theorem, the vector from the centre of one weft yarn to the centre of an adjacent weft yarn makes a 30° angle to the plane of the fabric.

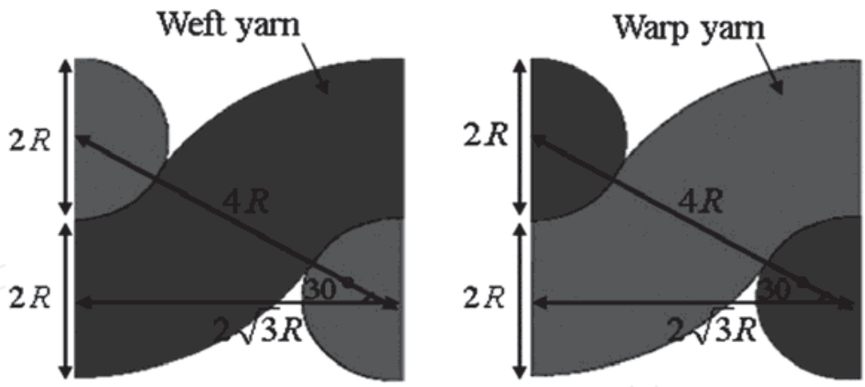

Fig. 6. Cross-section views of a plain woven fabric (source: Lee and Owens, 2011)

Using the flux integral, the area of one yarn in the unit fabric is calculated as:

$$r(u,v) = (2R + Rcosv)cosui + (2R + Rcosv)sinuj + Rcosvk \tag{20}$$

$$\left|r_u \times r_v\right| = R(2R + Rcosv) \tag{21}$$

$$A_{\text{yarn in unit area}} = \frac{\int_0^{2\pi}\int_0^{2\pi} R(2R + Rcosv)dudv}{3} = \frac{8\pi R^2}{3} \tag{22}$$

where R is the radius of yarn; A is the area; i, j and k are the vectors to x, y, and z axis direction, respectively; u and v are the notations for the variables of integration. Then, we determine the true fabric surface area as follows:

$$A_{\text{fabric}}^{\text{true}} = 2A_{\text{yarn in unit area}} = 52.64R^2 \tag{23}$$

where A^{true}_{fabric} is the intrinsic area of the unit fabric determined by the area of yarn surfaces. The apparent surface area is equal to the area of a plane tangent to the top surface.

$$A_{\text{fabric}}^{\text{apparent}} = \left(2\sqrt{3}R\right)^2 = 12R^2 \tag{24}$$

where $A^{apparent}_{fabric}$ is the apparent area of the unit fabric shown in Fig. 6. Finally, the roughness, r, is:

$$r = \frac{52.64R^2}{12R^2} = 4.39 \tag{25}$$

As shown in equation (25) the plain woven rough surface has high enough r to achieve a metastable CB surface.

Next, we look at a plain woven fabric made with multi-filament yarns. Clearly, a multi-filament yarn will have even higher values of r, because the space between the fibres will increase the true surface area whilst the apparent surface area remains the same. In this case, equation (23) becomes:

$$A_{\text{fabric}}^{\text{real}} = A_{\text{multi}} \approx 52.64R \times NR_f \tag{26}$$

where N is the number of filament fibres, R_y is the radius of the yarn, and R_f is the radius of the filament fibres. Substituting equation (26) into equation (25) yields:

$$r \approx 4.39\frac{NR_f}{R_y} \tag{27}$$

For example, a plan woven fabric could have, $R_y \approx 200$ μm, $N > 50$, and $R_f \approx 10$ μm. Substituting these values into equation (27) gives $r > 11$. Since $r > 11$ for the multi-filament fabric, we again expect that the surface is adequately rough and that the roughness is composed of the appropriate geometrical structures so as to be superhydrophobic.

Now, we model a Cassie-Baxter (CB) plain woven fabric. In Fig. 6, the centre-to-centre distance is $2\sqrt{3}R$ and the contact angle on a CB NyCo surface, θ_r^{CB}, is defined as:

$$\cos\theta_r^{CB} = \frac{(\pi - \theta_e)}{\sqrt{3}}\cos\theta_e + \frac{\sin\theta_e}{\sqrt{3}} - 1 \tag{28}$$

based on equation (11). Substituting Young contact angles into equation (28) along with the measured contact angles from the flat nylon film provides θ_r^{CB}. In addition, if the fabric consists of multi-filament yarns whose $D_f \sim R_f$, as shown in Fig 7, where R_f is the fibre radius and $2D_f$ is the distance between two adjacent fibres, the contact angle on CB multi-filament yarn, $\theta_r^{\text{multi-filament}}$, is defined as:

$$\cos\theta_r^{\text{multi-filament}} = \frac{(\pi - \theta_e)}{2}\cos\theta_e + \frac{1}{2}\sin\theta_e - 1 \tag{29}$$

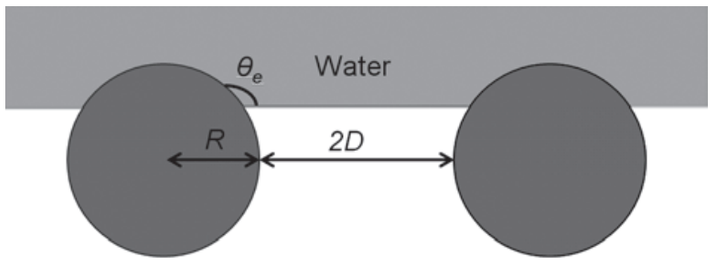

Fig. 7. A water droplet on two filament fibres

For $\theta_e > 90°$, θ_r^{CB} increases with increasing D. For example, if a fabric material is made of PTFE, ($\theta_e = 120°$) and the fibres are closely packed, $\theta_r^{CB} = 131°$; for D = R, $\theta_r^{CB} = 146°$; and for D = 2R, $\theta_r^{CB} = 152°$ on the multi-filament yarn.

As mentioned above, $109^o \le \theta_e$ (water) $\le 112^o$ and $73^o \le \theta_e$ (dodecane) $\le 75^o$ on a surface grafted with FS. By substituting these numbers into equation (28), we find $133° \le \theta_r^{CB}$ (water) $\le 136°$ and $98° \le \theta_r^{CB}$ (dodecane) $\le 100°$ for the FS-grafted mono-filament plain woven fabric. In the same manner, substituting the same θ_e into equation (29), we obtain $142° \le \theta_r^{\text{multi-filament}}$ (water) $\le 144°$ and $114° \le \theta_r^{\text{multi-filament}}$ (dodecane) $\le 115°$ for the FS-grafted multi-filament yarns. Using these values as the effective contact angles for the yarns in the plain woven structure and re-solving equation (28), i.e., substituting these values into θ_e (water) and θ_e (dodecane) in equation (28), we predict $161° \le \theta_r^{CB}$ (water) $\le 163°$ and $138° \le \theta_r^{CB}$ (dodecane) $\le 139°$ for the FS-grafted multi-filament plain woven fabric. According to our prediction, properly constructed NyCo multi-filament plain woven fabric can be

superhydrophobic and highly oleophobic once the fabric is treated with a low-surface-tension material such as FS.

2.3.2.2 Superhydrophobic oleophobic twill woven structure

Fig. 8 shows a cross-sectional view of a model of a NyCo twill woven fabric made of monofilament fibres. Flux integral can be used to obtain true area of twill woven fabric as well. The area of one yarn in the unit fabric is:

$$A_{\text{yarn in unit area}} = \frac{\int_0^{2\pi}\int_0^{2\pi} R(2R + R\cos v)\,du\,dv}{3} + \frac{\pi R^2}{2} = \left(\frac{8\pi^2}{3} + \frac{\pi}{2}\right)R^2 \tag{30}$$

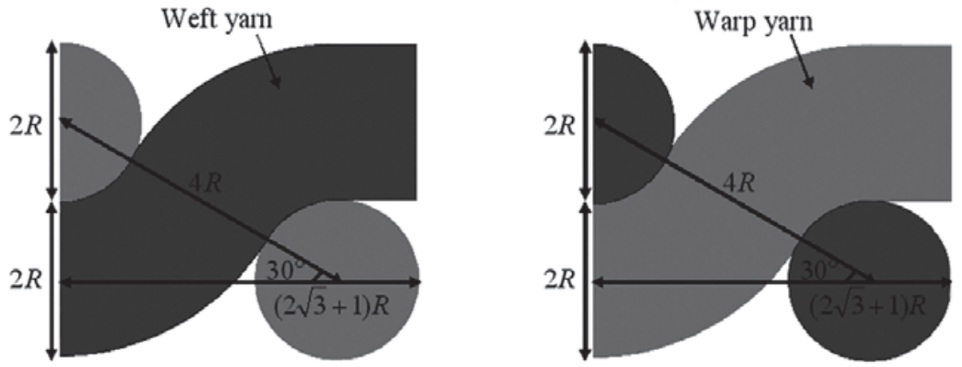

Fig. 8. Cross-section view of a twill woven fabric (source: Lee and Owens, 2010)

The area of one yarn in the unit fabric is applied to both weft and warp yarns, and a twill fabric in Fig. 8 consists of four yarns in the unit area. Therefore, the true fabric area is:

$$A_{\text{fabric}}^{\text{true}} = 4x\,A_{\text{yarn in unit area}} = 111.56R^2 \tag{31}$$

where $A^{\text{true}}_{\text{fabric}}$ is the intrinsic area of the unit fabric determined by the area of yarn surfaces. The apparent surface area is equal to the area of a plane tangent to the top surface.

$$A_{\text{fabric}}^{\text{apparent}} = \left[R(2\sqrt{3}+1)\right]^2 = 19.93R^2 \tag{32}$$

where $A^{\text{apparent}}_{\text{fabric}}$ is the apparent area of the unit fabric. Based on equation (10), the roughness, r, is 5.59. If this twill woven fabric is made of yarns having multi-filament fibres as shown in Fig 7, the fabric will have even higher values of roughness and r > 5.59, since the space between the fibres will increase the intrinsic surface area whilst the apparent surface area remains the same. Therefore, the twill woven rough surface has high enough r to exist as a metastable Cassie–Baxter surface regardless of the structure of yarns.

Now, we model a Cassie–Baxter twill woven fabric. In Fig. 8, the centre-to-centre distance is $(2\sqrt{3}+1)R$. Thus, a Cassie–Baxter NyCo surface is defined as:

$$\cos\theta_r^{CB} = \frac{4(\pi - \theta_e) + 1}{2\sqrt{3}+1}\cos\theta_e + \frac{4\sin\theta_e + 1}{2\sqrt{3}+1} - 1 \tag{33}$$

Substituting the same Young contact angles, $109^o \le \theta_e$ (water) $\le 112^o$ and $73^o \le \theta_e$ (dodecane) $\le 75^o$, into equation (29), we obtain $142° \le \theta_r^{\text{multi-filament}}$ (water) $\le 144°$ and $114° \le \theta_r^{\text{multi-filament}}$

(dodecane) ≤ 115° for the FS-grafted multi-filament yarns. Using these values as the effective contact angles for the yarns in the twill woven structure and re-solving equation (33), i.e., substituting these values into θ_e (water) and θ_e (dodecane) in equation (33), we predict 150° ≤ θ_r^{CB} (water) ≤ 152° and 118° ≤ θ_r^{CB} (dodecane) ≤ 119° for the FS-grafted multi-filament twill woven fabric. According to our prediction, properly constructed NyCo multi-filament twill woven fabric can also be superhydrophobic and highly oleophobic once the fabric is treated with a low-surface-tension material such as FS.

2.3.2.3 Superhydrophobic oleophobic satin woven structure

Fig. 9 shows a cross-sectional view of a model of a NyCo 3/1 stain woven fabric made from monofilament fibres. The surface area of a single round monofilament fibre in the unit fabric can be calculated using flux integral in order to obtain r as shown above.

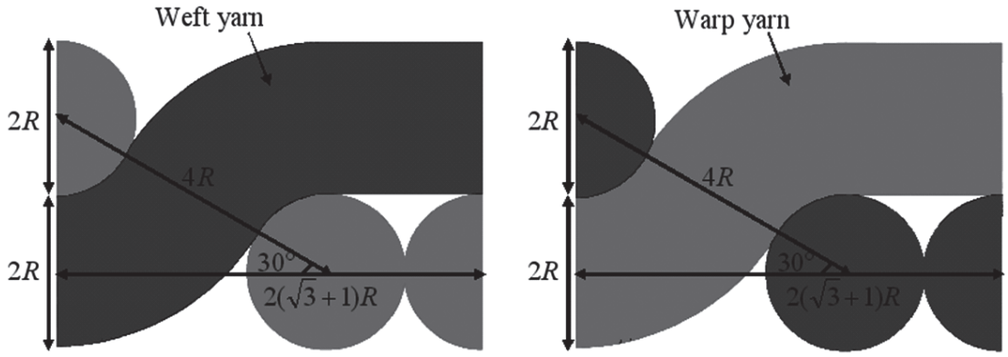

Fig. 9. Cross-section view of a 3/1 satin woven fabric

The area of one yarn in the unit fabric is:

$$A_{\text{yarn in unit area}} = \frac{\int_0^{2\pi}\int_0^{2\pi} R(2R + R\cos v)\,du\,dv}{3} + \pi R^2 = \left(\frac{8\pi^2}{3} + \pi\right)R^2 \tag{34}$$

The area of one yarn in the unit fabric is applied to both weft and warp yarns, and the satin fabric in Fig. 9 consists of six yarns in the unit area. Therefore, the true fabric area is:

$$A_{\text{fabric}}^{\text{real}} = 4\,A_{\text{yarn in unit area}} = 176.76R^2 \tag{35}$$

where A^{true}_{fabric} is the intrinsic area of the unit fabric determined by the area of yarn surfaces. The apparent surface area is equal to the area of a plane tangent to the top surface.

$$A_{\text{fabric}}^{\text{apparent}} = \left[2R(\sqrt{3}+1)\right]^2 = 29.85R^2 \tag{36}$$

where $A^{apparent}_{fabric}$ is the apparent area of the unit fabric. Based on equation (10), the roughness, r, is 5.92. If this satin woven fabric is made of yarns having multi-filament fibres as shown in Fig 9, the fabric will have even higher values of roughness and r > 5.92, since the space between the fibres will increase the intrinsic surface area whilst the apparent surface area remains the same. Therefore, the stain woven rough surface has high enough r to exist as a metastable Cassie–Baxter surface regardless of the structure of yarns.

Now, we model a Cassie–Baxter 3/1 satin woven fabric. In Fig. 9, the centre-to-centre distance is $(2\sqrt{3}+1)$R . Thus, a Cassie–Baxter NyCo surface is defined as:

$$\cos\theta_r^{CB} = \frac{2(\pi - \theta_e) + 1}{\sqrt{3}+1}\cos\theta_e + \frac{2\sin\theta_e + 1}{\sqrt{3}+1} - 1 \tag{37}$$

Again, substituting the same Young contact angles above, $109^o \le \theta_e$ (water) $\le 112^o$ and $73^o \le \theta_e$ (dodecane) $\le 75^o$, into equation (29), we obtain $142° \le \theta_r^{\text{multi-filament}}$ (water) $\le 144°$ and $114° \le \theta_r^{\text{multi-filament}}$ (dodecane) $\le 115°$ for the FS-grafted multi-filament yarns. Using these values as the effective contact angles for the yarns in the 3/1 satin woven structure and re-solving equation (37), we predict $149° \le \theta_r^{CB}$ (water) $\le 151°$ and $117° \le \theta_r^{CB}$ (dodecane) $\le 118°$ for the FS-grafted multi-filament 3/1 stain woven fabric. According to our prediction, properly constructed NyCo multi-filament satin woven fabric can also be superhydrophobic and highly oleophobic once the fabric is treated with a low-surface-tension material such as FS.

NyCo multi-filament woven fabric can be superhydrophobic but cannot be superoleophobic by itself, even if the fabric is treated with a low-surface-tension chemical. In order to achieve superoleophobicity as well as superhydrophobicity, the fabric morphology has to be manipulated by creating bigger spaces between fibres, loosening the fabric structure, or providing more roughness to the surface of NyCo multi-filament fibres. Considering the manufacturing process of woven fabrics, providing more roughness by adding protuberances to the surface of NyCo fibres seems the easiest way to achieve superhydrophobicity and superoleophobicity. Fig. 10 shows a NyCo surface covered with protuberances in micro and nano size FS. In the next section, we study how to create such a multi-scale roughness on the NyCo surface to prepare a metastable CB superhydrophobic and superoleophobic woven fabric.

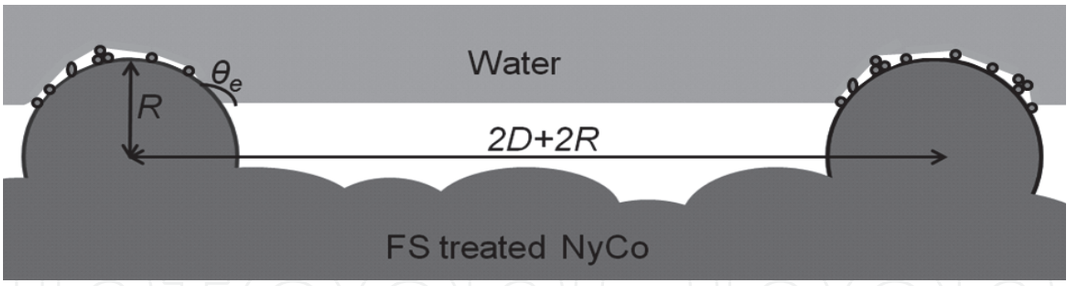

Fig. 10. A water drop on top of a NyCo fibre treated in a 10% FS solution consisting of base catalyst.

2.3.2.4 Superhydrophobic superoleophobic woven fabric

By using FS in conjunction with corrugated, rough surfaces, FS can build multi-scale roughness having low surface energy. Indeed, the previous research presented that the use of condensed silanes increases micro and nano structure corrugation and results in increased hydrophobicity and oleophobicity of so-treated cotton. A superhydrophobic and superoleophobic NyCo woven fabric can be developed in the same manner by covalently binding silanes onto the NyCo surface.

Although any soluble base can be an efficient catalyst, we use ammonium hydroxide as a base catalyst to accelerate the displacement of the methoxy or ethoxy substituent, and to facilitate the formation of the corrugated micro and nano-structure (Fig. 11).

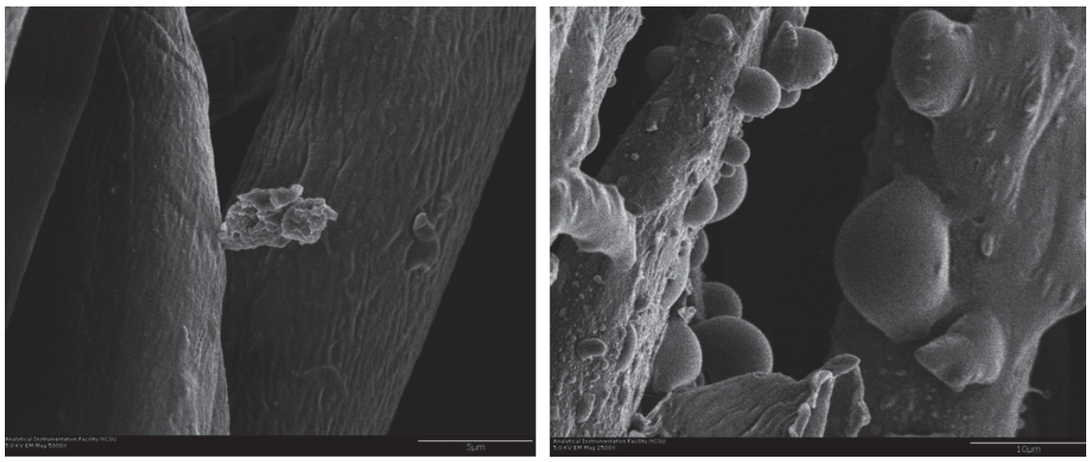

Fig. 11. Mult-scale protuberances on the FS-grafted NyCo surface. NyCo woven fabric was treated in a 10% solution of FS with catalytic water (left) and NyCo fibres treated in 10% FS with NH_4OH (right)

Since FS-treated NyCo without catalytic base has a relatively smooth surface whilst NyCo treated with FS in the presence of 1% catalytic base has multi-scale roughness on the surface, the X-ray photoelectron spectroscopy (XPS) of both FS treated NyCo with and without base catalyst was measured and compared with the XPS of untreated NyCo. Table 3 shows the XPS atomic composition of C, N, O, F, and Si and the ratio of F/O, F/C, and F/Si at the surface of three materials: (a) NyCo treated in a 10% solution of FS with catalytic water, (b) NyCo treated in a 10% solution of FS in the presence of 1% NH4OH, and (c) untreated NyCo. Both (a) and (b) have almost the same amount of fluorine regardless of the presence of base catalyst. However, as shown in Fig. 11, NyCo treated in a 10% solution of FS with water exhibits very different surface morphology compared to (b) although they possess almost the same atomic composition of F and nearly the same values of F/O, F/C, and F/Si ratios at the surface. As expected, based on the atomic composition of (c), the untreated NyCo does not have fluorine on the surface.

Fabric	Atomic composition (%)				Ratio		
	C	O	F	Si	F/O	F/C	F/Si
FS treated NyCo with water	39.1	8	50.2	2.7	6.3	1.3	18.4
FS treated NyCo with NH_4OH	38.4	8.6	50.5	2.5	5.9	1.3	20.4
Control NyCo	77	20.5	0	1.4	0	0	0

Table 3. XPS atomic composition of FS treated and untreated NyCo

By changing FS concentration, curing time, and the number of cures, we can control the morphology of FS protuberances on the NyCo surface and eventually prepare superhydrophobic and superoleophobic woven fabric (Fig. 12). The FS-treated NyCo plain woven fabric shown in Fig. 12 is superhydrophobic and superoleophobic. The fabric prevents the absorption of not only water but also dodecane with almost no change of contact angles.

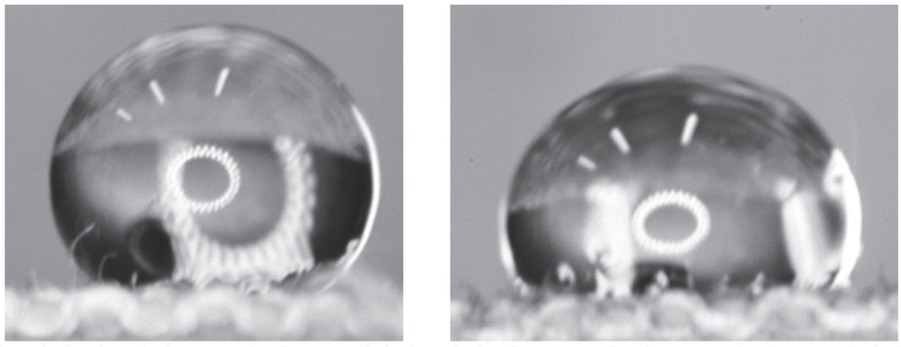

Fig. 12. 10 μL water (left) and dodecane (right) droplets sitting on top of FS-grafted NyCo plain woven fabric treated via microwave synthesis

The FS concentration, curing time, and the number of cures absolutely affect the wetting behaviour of FS-treated NyCo woven fabric. This indicates that oil contact angles can be greatly improved by varying such parameters. We suggest that improving the macro-scale geometric morphology of the woven fabric, such as controlling the fibre spacing, manipulating the yarn structure, and choosing the proper woven construction are also necessary to design and prepare superhydrophobic and superoleophobic fabrics.

3. Conclusion

In this chapter, we studied how to create superhydrophobic and superoleophobic woven fabric. A superhydrophobic superoleophobic surface is obtained by two criteria: a low surface tension and a properly designed rough surface having appropriate surface roughness and morphology. In order to make woven fabric superhydrophobic and superoleophobic, NyCo multi-filament plain woven fabric was treated with FS which has a very low surface tension and provides more roughness to the fabric by generating micro and nano-size protuberances in the form of FS condensates on the fibre surfaces. From the Young contact angles of water and dodecane on a FS-grafted nylon film, we could predict the apparent contact angles on FS-grafted NyCo multi-filament plain, twill, and 3/1 satin woven fabrics. Forming multi-scale geometric structure on the NyCo was also important to improve hydrophobicity and oleophobicity of the fabric, and consequently this treatment resulted in a highly hydrophobic and oleophobic woven fabric material. Finally, superhydrophobic superoleophobic plain woven fabric has been prepared using the Wenzel and the Cassie-Baxter equations. Although superoleophobicity is achieved via the metastable Cassie-Baxter model, the fabric can prevent the absorption of oil as well as water with almost no change of contact angles.

4. Acknowledgment

We appreciate support from the Defense Threat Reduction Agency-Joint Science and Technology Office for Chemical and Biological Defense (contract numbers BA07PRO102 and HDTRA1-08-1-0049) and Air Force Research Laboratory (grant number FA8650-07-1-5903). The U.S. Government is authorized to reproduce and distribute reprints for Governmental purposes notwithstanding any copyright notation thereon. The views and conclusions contained herein are those of the authors and should not be interpreted as necessarily

representing the official policies or endorsements, either expressed or implied, of Air Force Research Laboratory or the U. S. Government.

5. References

Balkenede, A. R, Boogaard, H. J. A. P. van de, Scholten, M., Willard, N. P. (1998), 'Evaluation of different approaches to assess the surface tension of low-energy solids by means of contact angle measurements', *Langmuir*, 14, 5907-5912.

Barton, A. F. M. (1983), *CRC Handbook of solubility parameters and other cohesion parameters*, Boca Raton, CRC Press, Inc.

Barthlott, W., Neihuis, C. (1997), 'Purity of the sacred lotus, or escape from contamination in biological surfaces', *Planta*, 202, 1-8.

Bico, J., Tordeux, C., Quere, D. (2001), 'Rough wetting', *Europhys Lett*, 55, 214-220.

Brar, T., France, P., Smirniotis, P. (2001), 'Heterogeneous versus homogeneous nucleation and growth of zeolite A', *J Phy. Chem B*, 105, 5383-5390.

Chhowalla, M., Amaratunga, G. A. J., Milne, W. I., McKinley, G. H., Gleason, K. K. (2003), ' Superhydrophobic carbon nanotube forests', *Nano Lett*, 3, 1701-1705.

Fowkes. F. M. (1963), 'Additivity of intermolecular forces at interfaces: I. Determination of the contribution to surface and interfacial tensions of dispersion forces in various liquids', *J Phys Chem*, 67, 2538-2541.

Fuerstner, R., Barthlott, W., Neinhuis, C., Walzel, P. (2005), 'Wetting and self-cleaning properties of artificial superhydrophobic surfaces', *Langmuir*, 21, 956-961.

Han, J. T., Xu, X., Cho, K. (2005), 'Diverse access to artificial superhydrophobic surfaces using block copolymers', *Langmuir*, 21, 6662-6665.

Hayn, R., Owens, J., Boyer, S., McDonald, R., Lee, H. (2011), 'Preparation of highly hydrophobic and oleophobic textile surfaces using microwave-promoted silane couling', *Journal of Materials Science*, 46, 2503-2509.

Hoefnagels, H., Wu, D., With, G., Ming, W. (2005), 'Biomimetic Superhydrophobic and Highly Oleophobic Cotton Textiles', *Langmuir*, 23, 13158-13163.

Jopp, J., Gruell, H., Yerushalmi-Rozen, R. (2004), 'Wetting behavior of water droplets on hydrophobic microtextures of comparable size', *Langmuir*, 20, 10015-10019.

Kim, J., Kim, C. (2002), 'Nanostructured surfaces for dramatic reduction of flow resistance in droplet-based microfluidics', *J Microelectromechanical System*, 11(5), 454-464.

Kim, S. H., Kim, J., Kang, B., Uhm, H. (2005), 'Superhydrophobic CF_x coating via in-line atmospheric RF plasma of He-CF_4-H_2', *Langmuir*, 21, 12213-12217.

Kovats, E. (1989), 'Wetting of low energy model surfaces', *Pure and App Chem*, 61, 1937-1944.

Krevelen, D. W. van, Hoftyzer, P. J. (1980), *Properties of Polymers*, New York, Elsvier/North-Holland Inc.

Krupenkin, T. N., Taylor, J. A., Schneider, T. M., Yang, S. (2004), 'From rolling ball to complete wetting: The dynamic tuning of liquids on nanostructured surface', *Langmuir*, 20, 3824-3827.

Kwong, V. H., Mossman, M. A., Whitehead, L. A. (2004), 'Control of reflectance of liquid droplets by means of electrowetting', *App Optics*, 43(4), 808-813.

Lau, K. K. S., Bico, J., Teo, K. B. K., Chhowalla, M., Amaratunga, G. J., Milne, W. I., McFinley, G. H., Gleason, K. K. (2003), 'Superhydrophobic carbon nanotube forests', *Nano Lett.*, 3, 1701-1705.

Lee, H., Michielsen, S. (2006), 'Lotus effect: superhydrophobicity', *Journal of Textile Institute*, 97, 455-462.

Lee, H., Owens J. (2010), 'Design of superhydrophobic ultraoleophobic nyco', *Journal of Materials Science*, 45, 3247-3253.

Lee, H., Owens J. (2011), 'Motion of liquid droplets on a superhydrophobic oleophobic surface', *Journal of Materials Science*, 46, 69-76.

Liu, H., Feng, L., Zhai, J., Jiang, L., Zhu, D. (2004), 'Reversible wettability of a chemical vapor deposition prepared ZnO film between superhydrophobicity and superhydrophilicity', *Langmuir*, 20, 5659-5661.

Marmur, A. (2004), 'The Lotus effect: superhydrophobicity and metastability', *Langmuir*, 20, 3517-3519.

McHale, G., Shirtcliffe, N. J., Newton, M. I. (2004), 'Contact-angle hysteresis on super-hydrophobic Surfaces', *Langmuir*, 20, 10146-10149.

Miwa, M., Nakajima, A., Fujishima, A., Hashimoto, K., Watanabe, T. (2004), 'Effects of the surface roughness on sliding angles of water droplets on superhydrophobic surfaces', *Langmuir*, 16, 5754-5760.

Nakajima, A., Hashimoto, K., Watanabe, T. (2005), 'Transparent superhydrophobic thin films with self-cleaning properties', *Langmuir*, 16, 7044-7047.

Ostrovskaya, L., Podesta, A., Milani, P., Ralchenko, V. (2003), 'Influence of surface morphology on the wettability of cluster-assembled carbon films', *Europhys Lett*, 63(3), 401-407.

Otten, A., Herminghaus, S. (2004), 'How plants keep dry: A physicist's point of view', *Langmuir*, 20, 2405-2408.

Pal, S. Weiss, H., Keller, H., Mueller-Plathe, F. (2005), 'Effect of nanostructure on the properties of water at the water-hydrophobic interface: a molecular dynamics simulation', *Langmuir*, 21, 3699-3709.

Patankar, N. A. (2003), 'On the modeling of hydrophobic contact angles on rough surfaces', *Langmuir*, 19, 1249-1253.

Roura, P., Fort, J. (2002), 'Comment on "Effects of the surface roughness on sliding angles of water droplets on superhydrophobic surfaces" ' *Langmuir*, 18, 566-569.

Sun, M., Luo, C., Xu, L., Ji, H., Ouyang, Q., Yu, D., Chen, Y. (2005), 'Artificial lotus leaf by nanocasting', *Langmuir*, 21, 8978-8981.

Sun, T., Feng, L., Gao, X., Jiang, L. (2005), 'Bioinspired surfaces with special wettability', *Acc Chem Res*, 38, 644-652.

Tadanaga, K., Morinaga, J., Matsuda, A., Minami, T. (2000), 'Superhydrohpobic-superhydrophilic micropatterning on flowerlike alumina coating film by the sol-gel method', *Chem Mater*, 12, 590-592.

Yoshimitsu, Z., Nakajima, A., Watanabe, T., Hashimoto, K. (2002), 'Effects of surface structure on the hydrophobicity and sliding behavior of water droplets', *Langmuir*, 18, 5818-5822.

Zhai, L., Cebeci F. C., Robert E. C., Rubner M. F. (2004), 'Stable superhydrophobic coatings from polyelectrolyte multilayers', *Nano Lett*, 4, 1349-1353.

Zhang, X., Sato, O., Taguchi, M., Einaga, Y., Murakami, T., Fujishima, A. (2005), 'Self-cleaning particle coating with antireflection properties', *Chem Mater*, 17, 696-700.

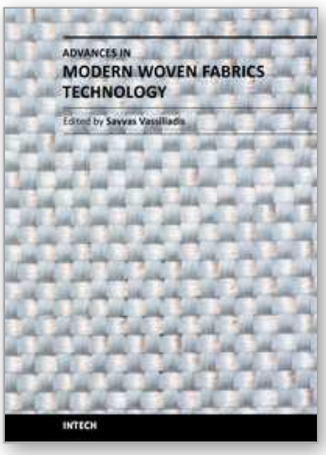

Advances in Modern Woven Fabrics Technology

Edited by Dr. Savvas Vassiliadis

ISBN 978-953-307-337-8
Hard cover, 240 pages
Publisher InTech
Published online 27, July, 2011
Published in print edition July, 2011

The importance of woven fabrics increases constantly. Starting from traditional uses mainly in clothing applications, woven fabrics today are key materials for structural, electronic, telecommunications, medical, aerospace and other technical application fields. The new application fields of the woven fabrics is directly reflected in the contents of the book. A selected collection of papers in the technological state-of-the-art builds the book â€œAdvances in Modern Woven Fabrics Technologyâ€. It is written by internationally recognized specialists and pioneers of the particular fields. The chapters embrace technological areas with major importance, while maintaining a high scientific level. This interdisciplinary book will be useful for the textile family member as well as for the experts of the related engineering fields. The open access character of the book will allow a worldwide and direct access to its contents, supporting the members of the academic and industrial community.

How to reference

In order to correctly reference this scholarly work, feel free to copy and paste the following:

Hoon Joo Lee and Jeffery Owens (2011). Superhydrophobic Superoleophobic Woven Fabrics, Advances in Modern Woven Fabrics Technology, Dr. Savvas Vassiliadis (Ed.), ISBN: 978-953-307-337-8, InTech, Available from: http://www.intechopen.com/books/advances-in-modern-woven-fabrics-technology/superhydrophobic-superoleophobic-woven-fabrics

INTECH
open science | open minds

InTech Europe
University Campus STeP Ri
Slavka Krautzeka 83/A
51000 Rijeka, Croatia
Phone: +385 (51) 770 447
Fax: +385 (51) 686 166
www.intechopen.com

InTech China
Unit 405, Office Block, Hotel Equatorial Shanghai
No.65, Yan An Road (West), Shanghai, 200040, China
中国上海市延安西路65号上海国际贵都大饭店办公楼405单元
Phone: +86-21-62489820
Fax: +86-21-62489821

IntechOpen